Magnetic field reversal of electric polarization and magnetoelectric phase diagram of the hexaferrite Ba1.3Sr0.7Co0.9Zn1.1Fe10.8Al1.2O22

Shipeng Shen, Liqin Yan, Yisheng Chai, Junzhuang Cong, and Young Sun

Citation: Applied Physics Letters **104**, 032905 (2014); doi: 10.1063/1.4862690
View online: http://dx.doi.org/10.1063/1.4862690
View Table of Contents: http://scitation.aip.org/content/aip/journal/apl/104/3?ver=pdfcov
Published by the AIP Publishing

This article is copyrighted as indicated in the article. Reuse of AIP content is subject to the terms at: http://scitation.aip.org/termsconditions. Downloaded to IP: 211.47.120.134 On: Wed, 22 Jan 2014 00:56:53

Magnetic field reversal of electric polarization and magnetoelectric phase diagram of the hexaferrite $Ba_{1.3}Sr_{0.7}Co_{0.9}Zn_{1.1}Fe_{10.8}Al_{1.2}O_{22}$

Shipeng Shen, Liqin Yan, Yisheng Chai, Junzhuang Cong, and Young Sun[a)]
Beijing National Laboratory for Condensed Matter Physics, Institute of Physics, Chinese Academy of Sciences, Beijing 100190, China

(Received 24 December 2013; accepted 7 January 2014; published online 21 January 2014)

Low magnetic field reversal of electric polarization has been demonstrated in the multiferroic Y-type hexaferrite $Ba_{1.3}Sr_{0.7}Co_{0.9}Zn_{1.1}Fe_{10.8}Al_{1.2}O_{22}$ single crystal. The maximum magnetoelectric coefficient at 200 K reaches 1065 ps/m near zero magnetic field. By a systematic investigation of magnetic field dependence of magnetic and dielectric responses at various temperatures, we obtained the magnetoelectric phase diagram describing the detailed evolution of the spin-induced ferroelectric phases with temperature and magnetic field. Below 225 K, the transverse spin cone can be stabilized at zero magnetic field, which is responsible for the reversal behavior of electric polarization. Our study reveals how to eventually achieve magnetic field reversal of electric polarization in hexaferrites at room temperature. © *2014 AIP Publishing LLC*. [http://dx.doi.org/10.1063/1.4862690]

The interplay between magnetic and ferroelectric orders in multiferroic materials has attracted a lot of research interest due to its potentials for advanced magnetoelectric (ME) devices as well as the intriguing physics.[1–9] Extensive researches have particularly focused on the spin-driven ferroelectrics[10]—the so-called ME multiferroic—in which the ferroelectric polarization (P) is induced by magnetic orders via the spin-current,[11] d-p hybridization,[12] or exchange striction mechanisms.[13,14] Among all the ME multiferroics, the hexaferrites have been considered as one of the very promising systems due to their giant ME effects up to room temperature.[15–19] Especially, in some of the multiferroic Y-type hexaferrites, the P can be reversed by a low magnetic field ($H < 300$ Oe),[20,21] which is very useful for the ME devices.

The multiferroic Y-type hexaferrites have the general chemical formula of $Ba_xSr_{2-x}Me_2Fe_{12}O_{22}$ ($Me = Co^{2+}$, Zn^{2+}, Ni^{2+}, etc.) with R-3 m space group.[15,16,20–23] The magnetic structures are composed of alternating L and S spin blocks stacking along the [001] direction,[24] as shown in Fig. 1(a). After zero magnetic field cooling (ZFC) process, they usually have incommensurate proper screw or incommensurate longitudinal conical spin ordering without hosting any ferroelectricity (FE).[25–27] By applying finite external in-plane H, a rich magnetic phase diagram is introduced. Especially, a kind of commensurate transverse conical spin configurations can be induced by H, as shown in Fig. 1(b). This phase is accompanied by FE up to room temperature, which can be explained by the spin current model $\boldsymbol{P} \propto \boldsymbol{k}_0 \times (\boldsymbol{S}_i \times \boldsymbol{S}_j)$, where $\boldsymbol{S_i}$ and $\boldsymbol{S_j}$ denote the neighbor spins at site i and j, $\boldsymbol{k_0}$ // [001] is the magnetic propagation vector.[11] According to this model, the screw or longitudinal conical spin configurations cannot generate $\boldsymbol{P}$ due to spin chirality $\sum(\boldsymbol{S}_i \times \boldsymbol{S}_j)$ // $\boldsymbol{k}_0$. However, after the field cooling (FC) process, the high field commensurate spin configurations can be maintained in some Y-type hexaferrites even in zero magnetic field, which is distinguished from the incommensurate spin configurations in the ZFC process. Consequently, the H-induced FE phases can also persist in zero-H and a continuous $\boldsymbol{P}$ reversing by the in-plane H is exhibited, indicating the spin chirality $\sum(\boldsymbol{S}_i \times \boldsymbol{S}_j)$ is preserved during the H reversal process.

Unfortunately, there are only very few Y-type hexaferrites demonstrating the P reversal by H and most of them occur at very low temperatures (T).[20,21] Recently, our group found the reversal of P by small H in the polycrystalline Y-type hexaferrite $BaSrCoZnFe_{11}AlO_{22}$ up to 250 K.[28] However, it is still unclear what determines the reversal behavior of P as a function of T and H. This information is crucial for understanding the physics as well as for exploring the low-field ME effects above room temperature. In this work, we have performed a systematic study of the spin-induced FE phase of a multiferroic Y-type hexaferrite single crystal in a wide range of H and T. The ME phase diagram obtained reveals that the reversal of P by H is critically related to the stabilization of the transverse cone spin configuration at zero H.

Single-crystal samples of the Y-type hexaferrites with a nominal composition of $BaSrCoZnFe_{11}AlO_{22}$ were grown from Na_2O-Fe_2O_3 flux in air.[29] The single crystal x-ray diffraction measurement was performed at room temperature using a x-ray diffractometer (Rigaku). The diffraction pattern proved a single-phase Y-type hexaferrite with $c = 43.28$ Å, as shown in Fig. 1(c). Energy dispersive spectrometry study reveals that the real chemical composition of the sample is $Ba_{1.3}Sr_{0.7}Co_{0.9}Zn_{1.1}Fe_{10.8}Al_{1.2}O_{22}$. The as-grown single crystalline samples were annealed in O_2 atmosphere to reduce the oxygen vacancies and enhance the resistivity using the method proposed by Chai *et al.*[22] For electrical measurements, the crystals were cut into thin plates with the widest faces perpendicular to the [120] direction in the hexagonal setting and then were painted with sliver paste on the widest faces. The electrical and magnetic measurements were carried out in the commercial Physical Properties Measurement System (PPMS, Quantum Design) and Magnetic Properties Measurement System (MPMS, Quantum Design), respectively.

[a)]Author to whom correspondence should be addressed. Electronic mail: youngsun@iphy.ac.cn

 © 2014 AIP Publishing LLC

This article is copyrighted as indicated in the article. Reuse of AIP content is subject to the terms at: http://scitation.aip.org/termsconditions. Downloaded to IP: 211.47.120.134 On: Wed, 22 Jan 2014 00:56:53

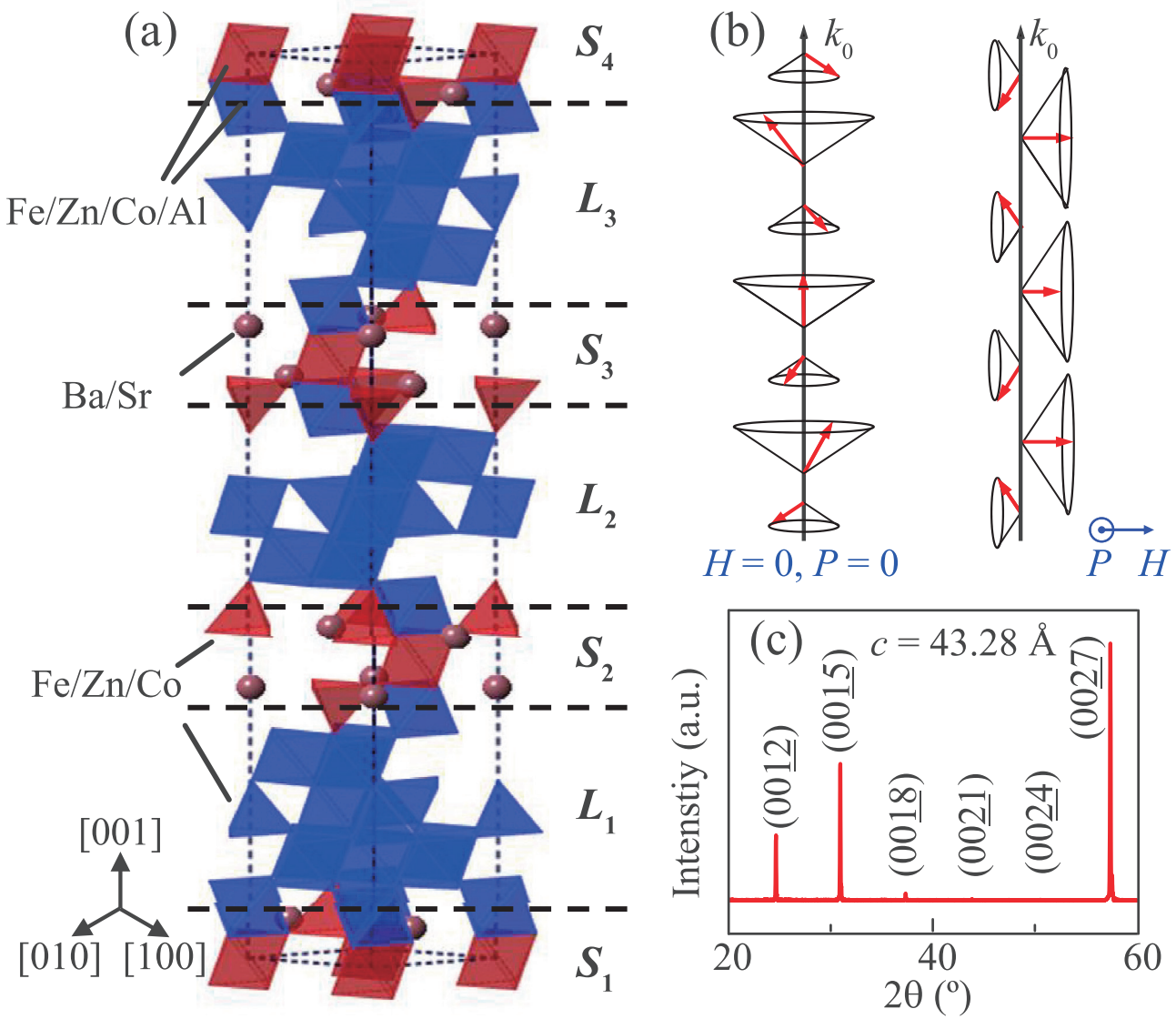

FIG. 1. (a) Schematic crystal structure of the Y-type hexaferrite $Ba_{1.3}Sr_{0.7}Co_{0.9}Zn_{1.1}Fe_{10.8}Al_{1.2}O_{22}$. The spin structure consists of alternate stacks of *L* blocks (blue) and *S* blocks (magenta) along [001] direction with large and small magnetic moments, respectively. (b) Schematic plots of the incommensurate longitudinal spin cone and the commensurate transverse spin cone states. (c) The X-ray diffraction pattern of the single crystal sample along [001] axis.

To measure the *H* dependent magnetoelectric currents at each temperature, we performed the magnetoelectric poling procedures: (1) At a fixed *T*, an electric field $E = 500$ kV/m was applied together with a high magnetic field of 70 kOe along [100] direction, which makes the sample in the paraelectric (PE) phase; (2) Then *H* was swept down to 5 kOe so as to drive the sample into the FE phase. After that, *E* was removed and the electrodes were shorted for 20 min; (3) Finally, the magnetoelectric currents were measured by an electrometer (Keithley 6517B) while sweeping *H* down to −70 kOe with the sweeping rate 80 Oe/s. The *P*-*H* curves were obtained by integrating the magnetoelectric currents as a function of time. Dielectric constant ε was measured by a LCR meter (Agilent 4980A) at 1 MHz frequency.

To study the magnetic properties of the $Ba_{1.3}Sr_{0.7}Co_{0.9}Zn_{1.1}Fe_{10.8}Al_{1.2}O_{22}$ single crystal, we start with the *M*-*H* measurements at 10 K to determine the field-driven magnetic ground states. As shown in Fig. 2(a), the in-plane virgin magnetization curve at 10 K after ZFC lies outside the hysteresis curve obtained in the subsequent field cycles. Such a behavior is typical in some multiferroic Y-type hexaferrites in which the in-plane *H* can drive the ZFC incommensurate spin state into a metastable commensurate transverse cone state. More importantly, with decreasing *H*, this transverse cone can be persisted at zero field, leading to an irreversible *M*-*H* curves.[21] Therefore, the in-plane *H* is very likely to induce a commensurate transverse cone spin configuration at 10 K near zero-*H* in the studied Y-type hexaferrite.

Then, we measured the *T* dependence of magnetization *M* in $H = 100$ Oe applied parallel and perpendicular to the [001] direction between 10 and 370 K, as shown in Fig. 2(b). Before the *M*-*T* measurements, an external $H = 10$ kOe was first applied at 10 K to induce the commensurate transverse cone state, and then ramped down to 100 Oe. It is very clear that the [001] direction is the magnetic hard axis below 370 K. For the in-plane *H* configuration, two magnetic transitions around 228 and 359 K can be clearly seen from the d*M*/d*T* vs *T* plot. Below 228 K, the magnetic phase remains the transverse cone state. Near 228 K, the magnetization decreases drastically, indicating that the transverse cone is

This article is copyrighted as indicated in the article. Reuse of AIP content is subject to the terms at: http://scitation.aip.org/termsconditions. Downloaded to IP: 211.47.120.134 On: Wed, 22 Jan 2014 00:56:53

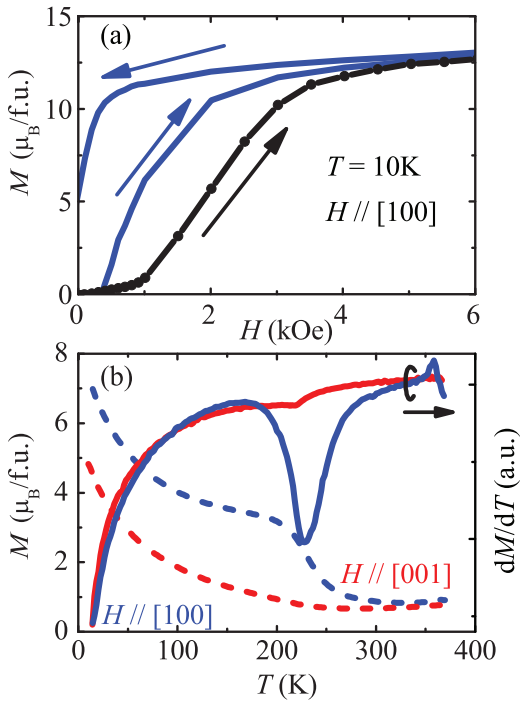

FIG. 2. (a) The magnetization as a function of magnetic field at 10 K. Dark closed circle and line indicate the virgin magnetization process. (b) The magnetization M and its derivative dM/dT as a function of temperature in $H = 100$ Oe along [100] and [001] directions, respectively. Before the measurements, $H = 10$ kOe was applied at 10 K to induce a metastable commensurate transverse cone state, then H was ramped down to 100 Oe.

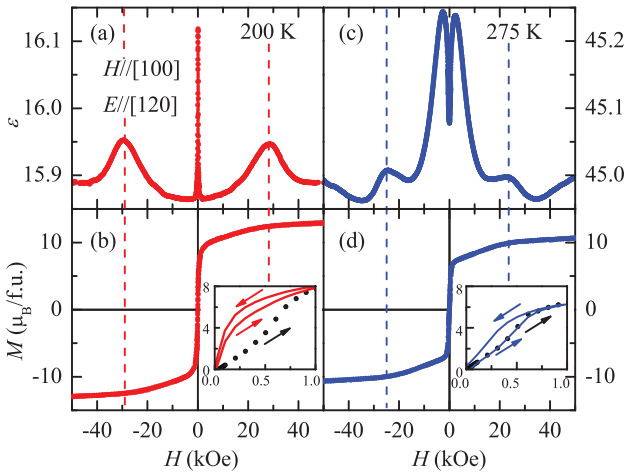

FIG. 3. H dependence of (a) dielectric constant ε and (b) magnetization M at 200 K. The inset of (b) shows the M-H curve at 200 K. Dark closed circle indicates the virgin magnetization process. H dependence of (c) ε and (d) M at 275 K. The inset of (d) presents the M-H curve at 275 K. Dark closed circle indicates the magnetization process. The arrows indicate the direction of scanning H.

replaced by a new spin configuration with smaller in-plane magnetization. Upon further increasing the temperature, a ferrimagnetic phase emerges above 359 K, which is similar to other reported hexaferrites.[15,20] For H // [001] configuration, the dM/dT curve only shows a very weak transition at 220 K while there is no clear transition around 359 K. The different transition temperatures between in-plane and out-of-plane configurations suggest that the magnetic field history and direction are crucial for spin configurations in the $Ba_{1.3}Sr_{0.7}Co_{0.9}Zn_{1.1}Fe_{10.8}Al_{1.2}O_{22}$ single crystal.

To further study the magnetic transition around 228 K, we measured the in-plane H dependent magnetic and dielectric properties at 200 and 275 K. The dielectric constant shows a broad peak at high magnetic field region ($|H| > 20$ kOe) at both 200 and 275 K, as shown in Figs. 3(a) and 3(c). Accordingly, the magnetization curve presents a kink at the same H, as shown in Figs. 3(b) and 3(d). These high-field features mark the phase transition between the paraelectric ferrimagnetic phase and the ferroelectric transverse cone phase in $Ba_{1.3}Sr_{0.7}Co_{0.9}Zn_{1.1}Fe_{10.8}Al_{1.2}O_{22}$, as indicated by previous studies of hexaferrites.[15,16,28] Thus, the transverse cone can persist under relatively large H at both temperatures. However, in the low field region, the magnetic and dielectric behaviors are quite different between two temperatures. At 200 K, there is a single dielectric peak centered at zero-H while two dielectric peaks at finite H ($\sim \pm 2$ kOe) are observed at 275 K. The low field M-H curves are also distinguished between two temperatures. As shown in the insets of Fig. 3, the virgin magnetization curve at 200 K lies outside the subsequent field cycle curve, very similar to that at 10 K. In contrast, the virgin curve is identical with the subsequent cycle curve at 275 K. Therefore, it strongly implies that the spin transverse cone persists down to zero-H at 200 K but a different zero-H phase appears at 275 K. It seems that a single dielectric peak at zero-H is a hallmark for the zero-H transverse cone phase while the finite low field peak at 275 K marks a FE to PE phase transition.

We also measured the H dependent $\varepsilon(H)$ and $M(H)$ in the intermediate temperatures. Fig. 4(a) shows the relative change of magnetodielectric $\Delta\varepsilon(H)/\varepsilon(10\text{ kOe}) = [\varepsilon(H) - \varepsilon(10\text{ kOe})]/\varepsilon(10\text{ kOe})$ with in-plane H sweeping from 10 to -10 kOe between 30 and 275 K. Below 225 K, there are only single dielectric constant peaks with a large magnetodielectric effect, $\Delta\varepsilon(H)/\varepsilon(10\text{ kOe}) = 1.6\%$ near zero-H. At 225 K, the peak value quickly decreases to 0.5% and a slight shoulder feature starts to appear at finite H. With further increasing the temperature, the intensity of the zero-H peak decreases gradually and the height of the shoulders at finite

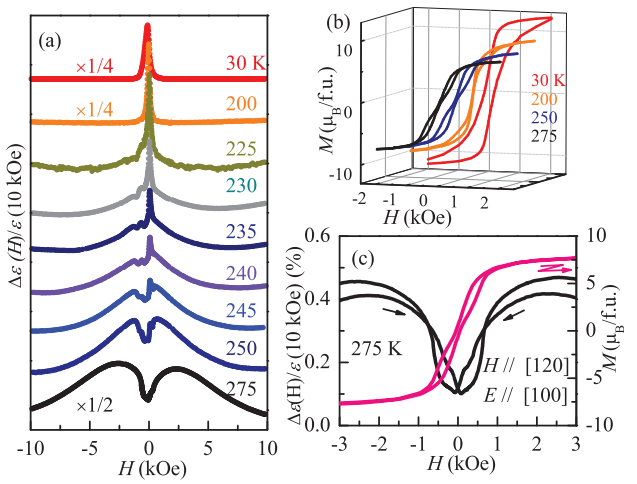

FIG. 4. (a) $\Delta\varepsilon(H)/\varepsilon(10\text{ kOe}) = [\varepsilon(H) - \varepsilon(10\text{ kOe})]/\varepsilon(10\text{ kOe})$ at low magnetic fields at selected temperatures. (b) The M-H curves in the low magnetic field region at selected temperatures. (c) The M-H and $\Delta\varepsilon(H)/\varepsilon(10\text{ kOe})$-$H$ curves around zero field at 275 K.

This article is copyrighted as indicated in the article. Reuse of AIP content is subject to the terms at: http://scitation.aip.org/termsconditions. Downloaded to IP: 211.47.120.134 On: Wed, 22 Jan 2014 00:56:53

H increases simultaneously. At 275 K, the zero-H single peak completely disappears and has been replaced by the double peaks around $H = \pm 2$ kOe. The suppression of zero-H dielectric peak with increasing temperature reflects the gradual disappearance of transverse cone phase. This tendency can also be reflected in the M-H curves, as shown in Fig. 4(b). Below 225 K, the magnetizations show abrupt reversal with very large slope at zero-H. However, above 225 K, the M-H curves display the S-like profile near zero-H, leading to a smaller slope at zero-H while the slope at finite H becomes larger. Especially, at $T = 275$ K where the M-H curve has larger slopes, the $\Delta\varepsilon(H)/\varepsilon(10\ \text{kOe})$ shows some anomalies instead of the peak near zero H, as shown in Fig. 4(c). From the above results, we conclude that there is a mixed magnetic phase in the low field region between 225 and 250 K.

It is found that if the commensurate transverse cone phase is stabilized at $H = 0$, the P can be reversed completely with the reversal of in-plane H due to the clamp of M and P order parameters. Thus, the $Ba_{1.3}Sr_{0.7}Co_{0.9}Zn_{1.1}Fe_{10.8}Al_{1.2}O_{22}$ single crystal should present P reversal by H below 228 K. We performed the in-plane H dependent polarization measurements by passing through the zero-H continuously, as shown in Fig. 5(a). The polarization can be indeed reversed by very small in-plane H up to 200 K. In this case, the single dielectric peak at zero-H should come from P reversal process. Above 200 K, because of the low resistivity of our crystal at high temperature, it is impossible to pole the sample to obtain reliable P-H curves. However, we speculate that the polarization would not be reversed totally by H above 228 K due to the phase mixing around zero-H. Above 275 K, polarization will disappear at $H = 0$ during H reversal due to the existence of a PE phase at the low-field region.

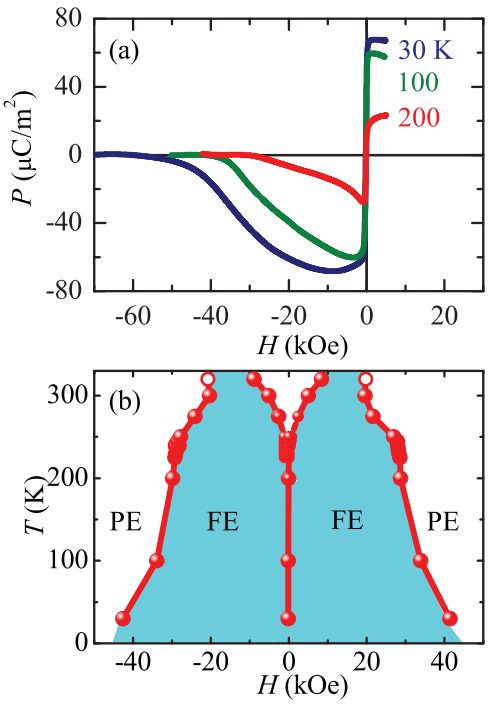

FIG. 5. (a) Magnetic field reversal of electric polarization at selected temperatures. (b) The magnetoelectric phase diagram of $Ba_{1.3}Sr_{0.7}Co_{0.9}Zn_{1.1}Fe_{10.8}Al_{1.2}O_{22}$. The phase boundaries are determined from the critical fields where the dielectric constant shows a peak with decreasing H.

Based on the ε-H and P-H curves at the selected temperatures up to 320 K, we obtained the phase boundaries of the spin-induced FE phase and plot the magnetoelectric phase diagram of $Ba_{1.3}Sr_{0.7}Co_{0.9}Zn_{1.1}Fe_{10.8}Al_{1.2}O_{22}$, as shown in Fig. 5(b). Below 200 K, there is no PE phase at zero-H and the solid circle line indicates the magnetic field of the peak from ε-H where electric polarization can be reversed by H. Between 225 and 250 K, PE and FE phases are likely to coexist at zero-H due to the magnetic phase mixing. Above 250 K, the zero-H FE phase is replaced by a PE phase with possible proper screw or alternating longitudinal conical spin configuration. At 320 K, the high-field phase boundaries are not well-defined due to high-field dielectric peak merging into the low-field dielectric peak, indicated by empty dots. It can be seen that the highest temperature at which the reversal of P by H can be realized is no higher than 225 K in our sample. Nevertheless, its FE phase can exist at much higher temperature than room temperature, probably up to 359 K as indicated by the dM/dT-T curve in Fig. 2(b). Although the P reversal temperature is lower than our previous report in polycrystalline samples, it is still the highest temperature in any reported multiferroic single crystals. Furthermore, a maximum ME coefficient (dP/dH) of 1065 ps/m is obtained near zero-H at 200 K.

In summary, we have demonstrated the low H reversal of P up to 200 K in the Y-type hexaferrite $Ba_{1.3}Sr_{0.7}Co_{0.9}Zn_{1.1}Fe_{10.8}Al_{1.2}O_{22}$ single crystal, and obtained the detailed magnetoelectric phase diagram. While the multiferroic phase can exist above room temperature, the reversal of P by an in-plane H becomes possible only below 225 K where the magnetic-field induced FE phase persists at zero-H. This correlation reveals that the reversal behavior of P is critically related to the stabilization of the transverse spin cone at zero-H. Therefore, to eventually realize H reversal of P at room temperature, one needs to improve the critical temperature at which the transverse spin cone becomes unstable near zero-H. This could be achieved by a careful adjustment of the composition of Y-type hexaferrites.

This work was supported by the Natural Science Foundation of China under Grant Nos. 11104337 and 11374347 and the National Key Basic Research Program of China under Grant No. 2011CB921801.

[1]W. Eerenstein, N. D. Mathur, and J. F. Scott, Nature **442**, 759 (2006).
[2]J. F. Scott, Nature Mater. **6**, 256 (2007).
[3]Y. H. Chu, L. W. Martin, M. B. Holcomb, M. Gajek, S. J. Han, Q. He, N. Blake, C. H. Yang, D. K. Lee, W. Hu, Q. Zhan, P. L. Yang, A. F. Rodriguez, A. Scholl, S. X. Wang, and R. Ramesh, Nature Mater. **7**, 478 (2008).
[4]A. Kumar, I. Rivera, R. S. Katiyar, and J. F. Scott, Appl. Phys. Lett. **92**, 132913 (2008).
[5]D. A. Sanchez, N. Ortega, A. Kumar, R. Roque-Malherbe, R. Polanco, J. F. Scott, and R. S. Katiyar, AIP Adv. **1**, 042169 (2011).
[6]J. F. Scott, NPG Asia Mater. **5**, e72 (2013).
[7]S. Mukherjee, A. Roy, S. Auluck, R. Prasad, R. Gupta, and A. Garg, Phys. Rev. Lett. **111**, 087601 (2013).
[8]L. Keeney, T. Maity, M. Schmidt, A. Amann, N. Deepak, N. Petkov, S. Roy, M. E. Pemble, and R. W. Whatmore, J. Am. Ceram. Soc. **96**, 2339 (2013).
[9]D. M. Evans, A. Schilling, A. Kumar, D. Sanchez, N. Ortega, M. Arredondo, R. S. Katiyar, J. M. Gregg, and J. F. Scott, Nat. Commun. **4**, 1534 (2013).
[10]T. Kimura, T. Goto, H. Shintani, K. Ishizaka, T. Arima, and Y. Tokura, Nature **426**, 55 (2003).

This article is copyrighted as indicated in the article. Reuse of AIP content is subject to the terms at: http://scitation.aip.org/termsconditions. Downloaded to IP: 211.47.120.134 On: Wed, 22 Jan 2014 00:56:53

[11]H. Katsura, N. Nagaosa, and A. V. Balatsky, Phys. Rev. Lett. **95**, 057205 (2005).
[12]T.-h. Arima, J. Phys. Soc. Jpn. **76**, 073702 (2007).
[13]S. Agrestini, L. C. Chapon, A. Daoud-Aladine, J. Schefer, A. Gukasov, C. Mazzoli, M. R. Lees, and O. A. Petrenko, Phys. Rev. Lett. **101**, 097207 (2008).
[14]L. C. Chapon, P. G. Radaelli, G. R. Blake, S. Park, and S. W. Cheong, Phys. Rev. Lett. **96**, 097601 (2006).
[15]T. Kimura, G. Lawes, and A. P. Ramirez, Phys. Rev. Lett. **94**, 137201 (2005).
[16]S. H. Chun, Y. S. Chai, Y. S. Oh, D. Jaiswal-Nagar, S. Y. Haam, I. Kim, B. Lee, D. H. Nam, K. T. Ko, J.-H. Park, J.-H. Chung, and K. H. Kim, Phys. Rev. Lett. **104**, 037204 (2010).
[17]Y. Kitagawa, Y. Hiraoka, T. Honda, T. Ishikura, H. Nakamura, and T. Kimura, Nature Mater. **9**, 797 (2010).
[18]S. H. Chun, Y. S. Chai, B.-G. Jeon, H. J. Kim, Y. S. Oh, I. Kim, H. Kim, B. J. Jeon, S. Y. Haam, J.-Y. Park, S. H. Lee, J.-H. Chung, J.-H. Park, and K. H. Kim, Phys. Rev. Lett. **108**, 177201 (2012).
[19]Y. Tokunaga, Y. Kaneko, D. Okuyama, S. Ishiwata, T. Arima, S. Wakimoto, K. Kakurai, Y. Taguchi, and Y. Tokura, Phys. Rev. Lett. **105**, 257201 (2010).
[20]S. Ishiwata, Y. Taguchi, H. Murakawa, Y. Onose, and Y. Tokura, Science **319**, 1643 (2008).
[21]H. B. Lee, S. H. Chun, K. W. Shin, B.-G. Jeon, Y. S. Chai, K. H. Kim, J. Schefer, H. Chang, S.-N. Yun, T.-Y. Joung, and J.-H. Chung, Phys. Rev. B **86**, 094435 (2012).
[22]Y. S. Chai, S. H. Chun, S. Y. Haam, Y. S. Oh, I. Kim, and K. H. Kim, New J. Phys. **11**, 073030 (2009).
[23]Y. Hiraoka, H. Nakamura, M. Soda, Y. Wakabayashi, and T. Kimura, J. Appl. Phys. **110**, 033920 (2011).
[24]N. Momozawa, Y. Yamaguchi, H. Takei, and M. Mita, J. Phys. Soc. Jpn. **54**, 771 (1985).
[25]H. Sagayama, K. Taniguchi, N. Abe, T.-h. Arima, Y. N. Shikawa, S.-i. Yano, Y. Kousaka, J. Akimitsu, M. Matsuura, and K. Hirota, Phys. Rev. B **80**, 180419 (2009).
[26]H. B. Lee, Y.-S. Song, J.-H. Chung, S. H. Chun, Y. S. Chai, K. H. Kim, M. Reehuis, K. Prokeš, and S. Mat'aš, Phys. Rev. B **83**, 144425 (2011).
[27]N. Momozawa and Y. Yamaguchi, J. Phys. Soc. Jpn. **62**, 1292 (1993).
[28]F. Wang, T. Zou, L. Q. Yan, Y. Liu, and Y. Sun, Appl. Phys. Lett. **100**, 122901 (2012).
[29]N. Momozawa, M. Mita, and H. Takei, J. Cryst. Growth **83**, 403 (1987).

This article is copyrighted as indicated in the article. Reuse of AIP content is subject to the terms at: http://scitation.aip.org/termsconditions. Downloaded to IP: 211.47.120.134 On: Wed, 22 Jan 2014 00:56:53